Atmospheric Environment 331 (2024) 120588

Contents lists available at ScienceDirect

Atmospheric Environment

journal homepage: www.elsevier.com/locate/atmosenv

Air quality and public health effects of dairy digesters in California

Jia Jiang [a,b], Yiting Li [c], Michael Kleeman [a,*]

[a] Department of Civil and Environmental Engineering, University of California, Davis, CA, 95616, United States
[b] Department of Civil and Environmental Engineering, Massachusetts Institute of Technology, Cambridge, MA, 02139, United States
[c] Department of Land, Air, and Water Resources, University of California, Davis, CA, 95616, United States

HIGHLIGHTS

- Dairy digesters capture methane from farms to reduce GHG emissions.
- Digesters configured to produce electricity increase local emissions of criteria pollutants.
- Widespread digester adoption would have minor effects on local air quality.
- Digesters do not harm public health or worsen air quality for disadvantaged communities.

ARTICLE INFO

Keywords:
Anaerobic digesters
$PM_{2.5}$
Ozone
BenMAP
Environmental justice

ABSTRACT

The dairy industry in California emits large amounts of methane (CH_4) that contributes significantly to the state's overall Greenhouse Gas (GHG) budget. Reducing CH_4 emissions has become a key priority for dairy farms in support of California's GHG reduction goals. Anaerobic digesters designed to capture CH_4 from animal manure present a practical option for reducing CH_4 emissions, but a comprehensive evaluation of the local air quality impacts of this technology has not been previously undertaken. The simplest digester configurations decrease local emissions of volatile organic compounds (VOCs) but increase emissions of oxides of nitrogen (NOx), potentially changing local air quality. Here, we evaluate the air quality implications of widespread digester adoption in the year 2050 across the San Joaquin Valley (SJV) in central California, which is home to the highest concentration of dairy farms in the state. Changes to concentrations of air pollutants including ozone (O_3), airborne particulate matter with diameter smaller than 2.5 μm ($PM_{2.5}$), and various $PM_{2.5}$ chemical components are predicted using the UCD/CIT chemical transport model at 4 km resolution. Dairy digester adoption is evaluated within two regional energy scenarios, including a business as usual (BAU) scenario and an 80% greenhouse gas reduction (GHGAi) scenario, to consider potential changes to the chemical regime that governs formation of secondary air pollution. Concentrations are evaluated across 32 randomly selected weeks over a 10-year period from the year 2046–2055 to establish a long-term average impact in the presence of El Niño Southern Oscillation (ENSO) variability. Regional weather patterns are downscaled from Global Climate Model simulations under the RCP8.5 global scenario. The results indicate that baseline dairy emissions make minor contributions to air pollutant concentrations in 2050. Under a worst-case scenario for digester adoption, $PM_{2.5}$ concentrations would increase by 0.06 $\mu g/m^3$ (current standard = 9 $\mu g/m^3$), and maximum daily 8-h average (MDA8) O_3 would change by −1.0 ppb to +0.2 ppb depending on the surrounding regional energy scenario (current standard = 70 ppb). A health impact analysis shows that the widespread use of dairy digesters would result in fewer than 0.1 additional deaths per 100,000 people due to changing air pollution. For comparison, this level of mortality change is more than 100 times smaller than the risk posed by seasonal flu. Further, Environmental Justice analysis indicates that the implementation of digesters will not influence the exposure disparities among different racial groups in either the SJV or the surrounding San Francisco Bay & Sacramento area. These findings suggest that dairy digesters can be widely adopted in central California to reduce GHG emissions with minimal effect on regional air quality and public health.

* Corresponding author.
E-mail address: mjkleeman@ucdavis.edu (M. Kleeman).

https://doi.org/10.1016/j.atmosenv.2024.120588
Received 14 February 2024; Received in revised form 13 May 2024; Accepted 16 May 2024
Available online 20 May 2024

1. Introduction

California is the leading dairy producer in the United States, with approximately 1.74M milk cows distributed across 1331 farms (CDFA, 2018) that contribute \$6.3B/yr to California's economy (CDFA, 2019). One out of every five cows in the United States lives in California. Dairy production in California emits significant quantities of greenhouse gases (GHGs), including methane (CH_4). The global warming potential of CH_4 is estimated to be 85 times larger than the warming potential of carbon dioxide (CO_2) over a 20-year timeframe (IEA, 2021). Almost all dairy farms in California feature manure lagoons where organic matter undergoes a biochemical degradation process that produces CH_4. Methane emissions from California dairies were equivalent to 118 million metric tons of carbon dioxide (MMTCO_2e) in 2013 (CARB, 2015), with dairy manure accounting for 25% of that total (29.5 MMTCO_2e) (El Mashad et al., 2023).

Anaerobic digesters, also referred to as dairy digesters, represent one possible measure to help mitigate CH_4 emissions from California dairies. Dairy digesters use microbes in a controlled environment to degrade the waste organic matter so that the CH_4 can be captured and used as a power source in many applications that would have otherwise used traditional fossil natural gas. Lifecycle analysis has shown that dairy digesters can reduce the GHG footprint of dairy farms by ~40% (El Mashad et al., 2023). One possible disadvantage of dairy digesters in California is their potential to exacerbate air pollution problems in the San Joaquin Valley (SJV) where most of the dairy production takes place. Capturing and using CH_4 produced by dairy digesters has the potential to increase criteria pollutant emissions around farms, which could exacerbate air quality problems near disadvantaged communities. Previous studies have examined the long-term environmental effects of methane control technologies, including dairy digesters (Anenberg et al., 2012; Fiore et al., 2002; Giorgi and Meleux, 2007; Mosavi, 2023; Staniaszek et al., 2022) but no study has comprehensively assessed the short-term air quality impacts of widespread digester adoption in an intensively farmed region like the SJV.

Dairy digesters can be configured and operated to produce CH_4 with various levels of purity. The simplest configuration produces "biogas" composed of approximately 50% CH_4, 50% CO_2, and trace amounts of other impurities that can be burned onsite to produce electricity. Widespread adoption of dairy digesters configured to produce electricity would effectively shift emissions of oxides of nitrogen (NOx) and airborne particulate matter with aerodynamic diameter smaller than 2.5 μm ($PM_{2.5}$) from traditional power plants to locations around dairy farms. Here, we analyze the potential air quality impacts of this "worst case" scenario by comparing to a business-as-usual scenario with traditional dairy emissions, and a hypothetical "perfect case" scenario in which dairy emissions are completely controlled using some currently-unknown technology. Each of these local SJV scenarios is analyzed within two regional energy scenarios for non-dairy sources that have the potential to influence the chemical regimes that govern pollution formation. The first regional energy scenario assumes business-as-usual emissions from non-agricultural sectors across California. The second regional energy scenario assumes the adoption of low-carbon energy sources in non-agricultural sectors across California. All "regional + dairy" scenarios are analyzed using a chemical transport model that accounts for pollution formation in the presence of emissions, transport, deposition, and chemical reactions in both the gas and condensed phases. Long-term average concentrations for O_3 and $PM_{2.5}$ in each "regional + dairy" scenario are compared in order to quantify the potential for dairy digesters to negatively impact air quality in the SJV. Exposures are summarized for the total population and for different race/ethnicity groups to investigate potential Environmental Justice concerns. The results determine the maximum impact that dairy digesters can have on air quality and public health across Central and Northern California.

2. Methodology

2.1. Air quality model

Future air pollution concentrations were predicted with the UCD/CIT air quality model configured with 4 km spatial resolution across Central and Northern California. The UCD/CIT air quality model has been used to predict air pollution concentrations in numerous past studies in California and across the U.S. (Akherati et al., 2019; Hu et al., 2015; Hu et al., 2017; Hu et al., 2019; Jerrett et al., 2023; Li et al., 2024; Venecek et al., 2018; Venecek et al., 2019; Yu et al., 2019; Zhao et al., 2022). Each of these studies included a comparison to measurements and statistical analysis based on typical CTM performance criteria (Emery et al., 2017). The UCD/CIT model has also been used to predict concentrations in multiple future climate and energy scenarios (Zhao et al., 2023; Li et al., 2023; Li et al., 2022a; Zapata et al., 2018b).

Large scale meteorological inputs were obtained from the Community Climate System Model (CCSM) (NCAR, 2011) under the Representative Concentration Pathway 8.5 (RCP8.5) (IPCC, 2014). The Weather Research and Forecasting (WRF) model v3.4. was used to downscale the fine scale meteorology. Biogenic emissions were predicted using the Model of Emissions of Gases and Aerosols from Nature (MEGAN) v2.1. It is noteworthy that our analysis did not incorporate wildfire emissions, under the assumption that these emissions would remain consistent across different dairy biogas scenarios, thereby not affecting the relative outcomes of our comparative analysis.

Simulations were conducted over 32 individual weeks (8 weeks/season), randomly selected from the year 2046–2055, each initiated with a three-day spin-up period, in order to accurately capture long-term average concentration levels while also accounting for meteorological fluctuations induced by the El Niño Southern Oscillation (ENSO). The simulated 32 weeks generate estimates for $PM_{2.5}$ exposure in central California that are within ± 0.75 μg/m^3 of the 10-yr average mean with 95% confidence. Furthermore, the changes in pollution exposure under different emissions scenarios are evaluated on the same days using identical meteorology, effectively removing any uncertainty associated with the choice of simulation periods.

2.2. Future emissions scenarios

2.2.1. Future regional energy scenario emissions inventories

Atmosphere chemistry is "non-linear" meaning that changes to emissions can sometimes increase or decrease ambient concentrations of chemical species depending on the atmospheric chemical regime. In this work, two regional energy scenarios (Table 1) were established to evaluate the potential changes to atmospheric concentrations that may yield different behaviors due to different chemical regimes. The two regional energy scenarios created for the year 2050 included a business as usual (BAU) scenario and an 80% GHG reduction (GHGAi) scenario (Li et al., 2022b). The differences in the future energy choices are sufficiently large to shift the atmospheric chemical regime from NOx-rich to NOx-limited in some locations. Since we cannot predict which

Table 1
Regional baseline energy scenario descriptions.

Regional energy scenario name	Description[a]
BAU	A business as usual scenario that includes current regulations and future growth projections.
GHGAi	A strict GHG reduction scenario that achieves an 80% reduction of GHG emissions (relative to 1990 levels) by the year 2050. More than 60% of California's primary energy is supplied by renewables, including biomass, wind, and solar.

[a] More details about the regional energy scenarios are in Zapata et al. (2018a, 2018b), and Li et al. (2022b).

future will come to pass, we choose to analyze the potential for dairy digester adoption under both possible future scenarios. Both the BAU and GHGAi regional energy scenarios were constructed using the energy-economic optimization model, CA-TIMES, that calculates the multi-sector energy portfolio that meets projected energy supply and demand at the lowest cost, while also satisfying scenario-specific GHG emissions constraints (Zapata et al., 2018b).

Corresponding criteria pollutant emissions for each regional energy scenario were spatially allocated at 4 km resolution to support air quality analysis across California with the CAREMARQUE model (Li et al., 2022b; Zapata et al., 2018b). CA-REMARQUE translates the changes to energy production predicted in CA-TIMES into changes in criteria pollutant emissions. The CA-REMARQUE model therefore extends the capabilities of the CA-TIMES model beyond GHGs. CA-REMARQUE modifies criteria pollutant emissions based on meteorology, most notably accounting for the influence of temperature on biogenic emissions and evaporative fuel emissions. Future emissions scenarios that adopt low-carbon energy use much less fossil fuel, making evaporative emissions minor, but temperature effects on biogenic emissions remain significant.

Earlier versions of CA-TIMES/CA-REMARQUE explicitly accounted for dairy biogas energy production (Zapata et al., 2018b), but later versions omitted the criteria pollutant emissions from this relatively minor source of energy (Li et al., 2022b). Neither the BAU or the GHGAi regional energy scenario accounted for development of dairy digesters as an energy source, and so digester adoption is treated as a perturbation to these regional energy scenarios in the current study. The amount of energy produced by complete digester adoption is small (~80 MW) relative to the statewide total electrical production (84,671 MW in 2022). It is assumed that digesters will replace fossil natural gas electrical generating units in the study region rather than other potential sources of electrical generation in order to fairly evaluate the tradeoffs involved.

CA-REMARQUE uses algorithms that account for local information about activity levels and technology mixes to estimate emissions of criteria pollutants (or their precursors) that are consistent with future scenarios. Emissions of criteria pollutants did not uniformly decrease in all sectors of the economy under each scenario. This resulted in non-uniform changes to criteria pollutant emissions close to densely populated areas, consequently affecting the level of air pollution that these populations are exposed to. As a further complication, changing fuels and technology also modified the composition of reactive organic gas (ROG) emissions as well as the size and composition of particulate matter emissions. This is most apparent when comparing the reductions in emissions for various size fractions of primary particulate matter; for instance, primary $PM_{2.5}$ emissions decrease by 3.6% in the GHGAi regional energy scenario versus the BAU regional energy scenario while corresponding primary $PM_{0.1}$ emissions decrease by a factor of 36% (Zapata et al., 2018b). For further information on the energy scenarios, refer to Zapata et al. (2018a, 2018b), and Li et al. (2022b).

2.2.2. Future dairy scenarios

Two limiting local dairy scenarios are explored to gain insights into the potential for future air quality impacts. A summary of these "regional + dairy" emissions scenarios is shown in Table 2, with further details discussed below.

2.2.2.1. Limiting dairy scenario 1: Perfect dairy control (Perfect-Control).

The first limiting emissions scenario assumes universal 100% control of all VOC, NH_3, and PM emissions from dairy waste. In reality, PM emissions from dairy farms are chiefly composed of dust generated by dairy cattle walking on unpaved surfaces. The perfect scenario quantifies the upper bound of the air quality improvements that could be achieved through the adoption of hypothetical new dairy control technologies in central California.

Table 2
Summary of emissions scenarios evaluated.

BAU regional energy & Dairy Perfect-Control	GHGAi regional energy & Dairy Perfect-Control
BAU regional energy & Dairy Biogas-Electricity	GHGAi regional energy & Dairy Biogas-Electricity

2.2.2.2. Limiting dairy scenario 2: Widespread biogas digesters with 100% adoption (Biogas-Electricity).

Biogas production using covered lagoon technology has advanced significantly in recent years. Multiple commercial companies have evolved business models that install and operate covered lagoons for biogas production on dairy farms yielding financial benefits for farm owners. These innovations have significantly lowered or eliminated the barriers to biogas production. The current analysis will focus on the digester configuration with the highest potential for air quality impacts: all farms adopt covered lagoon digesters with on-site electricity generation.

Biogas production at dairy facilities was assumed to eliminate emissions of dairy waste VOCs but otherwise leave emissions of NH_3 and PM from dairy waste unchanged. Biogas electricity production at dairy facilities generates new emissions of NOx and PM from the engines operating on biogas. Engine technology used for electricity generation was assumed to meet Tier 4 standards for diesel engines of 0.4 g NOx/kW/hr, and 0.02 g PM/kW/hr (EPAU.S, 2016). It should be noted that these levels are slightly lower than the currently permitted levels for biogas-fired engines in the SJV. The current calculations account for continued tightening of future standards and/or the incorporation of safety factors by engine manufacturers to avoid emissions violations. It was assumed that digesters would process 100% of the generated dairy waste, and that biogas production potential was proportional to the amount of dairy waste VOC emissions in the emissions inventory produced by the California Air Resources Board (CARB). Emissions records describing dairy waste were modified to remove evaporative VOC emissions and add NOx and PM emissions from dairy biogas combustion. The placement of the biogas combustion emissions assumes that the biogas production facilities would be located close to existing dairy barns so that existing spatial surrogates for dairy VOC emissions can also act to locate emissions from engines operating on dairy biogas.

Table 3 summarizes the emissions associated with dairy waste in California under the regional energy scenario (BAU or GHGAi) atmosphere, the Perfect-Control scenario, and the Biogas-Electricity scenario. Baseline emissions are estimated as the 2010 dairy waste emissions coded with EIC = 620-618-0262-0101 multiplied by a factor of 1.5 to represent increased demand in response to anticipated population growth by the year 2050 (Zapata et al., 2018a). The emissions of all particles and gases are eliminated under the Perfect-Control scenario as a limiting case study. Emissions are modified in the Biogas-Electricity scenario to account for removal of VOC emissions from the dairy waste and the addition of engine exhaust produced from burning the biogas (see Biogas Electricity column in Table 3). NOx emissions in the traditional natural gas sources were reduced in the Biogas-Electricity scenario to account for a shift of approximately 80 MW of electricity production from traditional plants to new biogas plants (see Biogas Electricity column in Table 3).

3. Results

3.1. Model predictions

3.1.1. Baseline concentration fields

Fig. 1 illustrates the baseline future concentrations of 99th percentile maximum daily 8-h average (MDA8) O_3 and annual average $PM_{2.5}$ mass predicted under the BAU regional energy scenario and the GHGAi regional energy scenario. Each concentration for the year 2050

Table 3
Daily emission totals associated with dairy waste under different scenarios.

Species	Baseline	Perfect-Control	Biogas-Electricity
Gas-Phase Species[a] (kmol/day)			
CO	0	0	1790
NOx	0	0	111
CH4	22,443	0[b]	1173
ALK1	3425	0	114
ALK2	0	0	16
ALK3	325	0	6
ALK4	171	0	1
ETHENE	0	0	6
OLE1	0	0	11
OLE2	0	0	2
ACETYLENE	0	0	3
HCHO	0	0	7
ACET	177	0	0
ETOH	198	0	0
NH3	9140	0	9140
Particle-phase Species (kg/day)			
EC[c]	0	0	1
OC[d]	1205	0	1219
CL^-	29	0	33
SO_4^{2-}	23	0	53
NO_3^-	47	0	48
METL	404	0	405
Mn	3	0	3
Fe	96	0	96
OTHER	2596	0	2610

[a] Gas-phase mechanism in UCD/CIT model is based on SAPRC-11 and detailed definition of the gas-phase model species can refer to Carter and Heo (2013).
[b] Limiting scenario assumption.
[c] Elemental (black) carbon (EC).
[d] Organic carbon (OC).

illustrated in Fig. 1 was calculated based on 32 simulated weeks (8 weeks/season) randomly distributed across a 10-year period between 2046 and 2055.

In both regional energy scenarios, the 99th percentile MDA8 O_3 concentration peaks over the Santa Clara Valley. This region has a high level of urbanization, heavy traffic, industrial activities, and meteorology that traps pollutants in its bowl-like topography. The maximum values of the 99th percentile MDA8 O_3 concentrations are approximately 70 ppb in the BAU regional energy scenario and 68 ppb in the GHGAi regional energy scenario. In contrast to the GHGAi regional energy scenario, the BAU regional energy scenario exhibits an additional concentration peak over the SJV and into the Sierra Nevada Mountain Range at the interface between urban NOx emissions and biogenic VOC emissions.

Long-term average $PM_{2.5}$ concentrations are predicted to reach 13–14 $\mu g/m^3$ in the regions surrounding major cities such as San Francisco and San Jose in the BAU regional energy scenario. In SJV, namely between Fresno and Bakersfield, the $PM_{2.5}$ concentration is expected to reach 15 $\mu g/m^3$. Furthermore, in the San Francisco Bay Area, the projected $PM_{2.5}$ concentrations are estimated to reach as high as 18 $\mu g/m^3$ around ports. The GHGAi regional energy scenario has a regional distribution of $PM_{2.5}$ concentrations that closely resembles that of the BAU regional energy scenario, although with concentrations 1–2 $\mu g/m^3$ lower. Notably, the most significant reduction in $PM_{2.5}$ concentrations is seen in the SJV area (Fig. S9).

The results illustrated in Fig. 1 show that the baseline atmospheric conditions are cleaner under the GHGAi regional energy scenario than the BAU regional energy scenario due to reduced emissions, particularly within the SJV. The reductions in the NOx and VOC emissions that lead to the cleaner atmosphere in the GHGAi regional energy scenario could potentially shift the atmospheric chemistry from a VOC-limited regime to a NOx-limited regime. This issue will be explored further in the following sections that examine how changes in dairy emissions influence O_3 and $PM_{2.5}$ concentrations.

3.1.2. O_3 response

Among the 32 simulated weeks, MDA8 O_3 concentrations exceed 70 ppb on 54 days under the BAU regional energy scenario and 19 days under the GHGAi regional energy scenario for the baseline conditions. In the BAU regional energy scenario, the perfect dairy control measures decrease the number of days with MDA8 O_3 levels exceeding 70 ppb, dropping them from 54 to 45 days. However, under the GHGAi regional energy scenario, the frequency of days with MDA8 O_3 concentrations exceeding 70 ppb remain unchanged when perfect dairy control is adopted. The changes in MDA8 O_3 levels under various future scenarios relative to the baseline concentrations are further illustrated in Fig. 2. Results are displayed for the average across all 32 simulated weeks, and the 99th percentile of MDA8 O_3 concentrations. Seasonal variations and detailed trends are provided in Supporting Information (SI).

Fig. 2 (a,b) shows the predicted change in annual mean and 99th percentile MDA8 O_3 concentrations under the Perfect-Control scenario where 100% of the dairy waste emissions are removed under a BAU regional energy scenario. MDA8 O_3 concentrations decrease across the entire SJV in response to removing dairy farm VOC emissions, with maximum reductions of 1 ppb for annual mean concentrations and 2.1 ppb for the 99th percentile MDA8 O_3 concentration. In Fig. S1, changes in the spring (MAM) are minimal, changes in the summer (JJA) and fall (SON) are approximately equal, while changes in fall are greatest.

Fig. 2 (c,d) shows predicted changes in MDA8 O_3 concentrations in response to the adoption of a Perfect-Control in a GHGAi regional energy scenario. The maximum changes observed in the annual mean concentrations are approximately 0.4 ppb. This is nearly half the magnitude of changes seen in the BAU regional energy scenario, as depicted in Fig. 2a. A similar trend is noted for the 99th percentile MDA8 O_3 concentration. The spatial and seasonal patterns of O_3 concentration changes attributable to the Perfect-Control scenario in the GHGAi regional energy scenario are similar to the BAU regional energy scenario but the magnitude of the changes is moderated.

Fig. 2 (e,f) shows predicted changes to MDA8 O_3 concentrations in the Biogas-Electricity scenario, responding to the widespread adoption of biogas production and electricity generation across dairy farms in the SJV under a BAU regional energy scenario. Emissions of traditional VOCs from dairy waste are eliminated under this scenario. Emissions of NOx and $PM_{2.5}$ are increased from the biogas combustion process and reduced at traditional natural gas electricity generation units. Predicted ambient concentrations of NOx in the SJV increase by approximately 0.15 ppb in response to increased NOx emissions from biogas combustion. The NOx emission in the traditional natural gas sources were reduced by a factor of 0.47 under the assumption that the biogas electricity generation exhibits a comparable level of NOx emissions per kWh as traditional natural gas electricity generation. This change in NOx concentrations is relatively minor and so the spatial pattern of changing O_3 concentrations under the Biogas-Electricity scenario is driven mostly by the reduction in the emissions of VOCs from dairy waste. The spatial pattern of changes to O_3 concentrations in the Biogas-Electricity scenario (Fig. 2 (e,f)) is therefore very similar to the spatial pattern predicted under the Perfect-Control scenario (Fig. 2 (a,b)), with the exception of a minor increase in the Sacramento region (below 0.1 ppb). The majority of the O_3 concentration reduction occurs in the agricultural region between Fresno and Bakersfield that has a large number of dairy farms. Maximum reductions in MDA8 O_3 concentrations are predicted to be 0.6–1.0 ppb.

Fig. 2 (g,h) shows changes to predicted MDA8 O_3 concentrations in the Biogas-Electricity scenario under a GHGAi regional energy scenario. While O_3 concentrations decrease in the SJV and San Francisco Bay Area, as observed in other scenarios, there is a slight increase in O_3 concentrations in the Sacramento Area in response to the increased NOx emissions from biogas combustion. NOx emissions decrease in surrounding fossil natural gas power plants, but the net change is a slight O_3 increase in Sacramento. This increase is most pronounced during the summer months (JJA), with the maximum value reaching 0.2 ppb

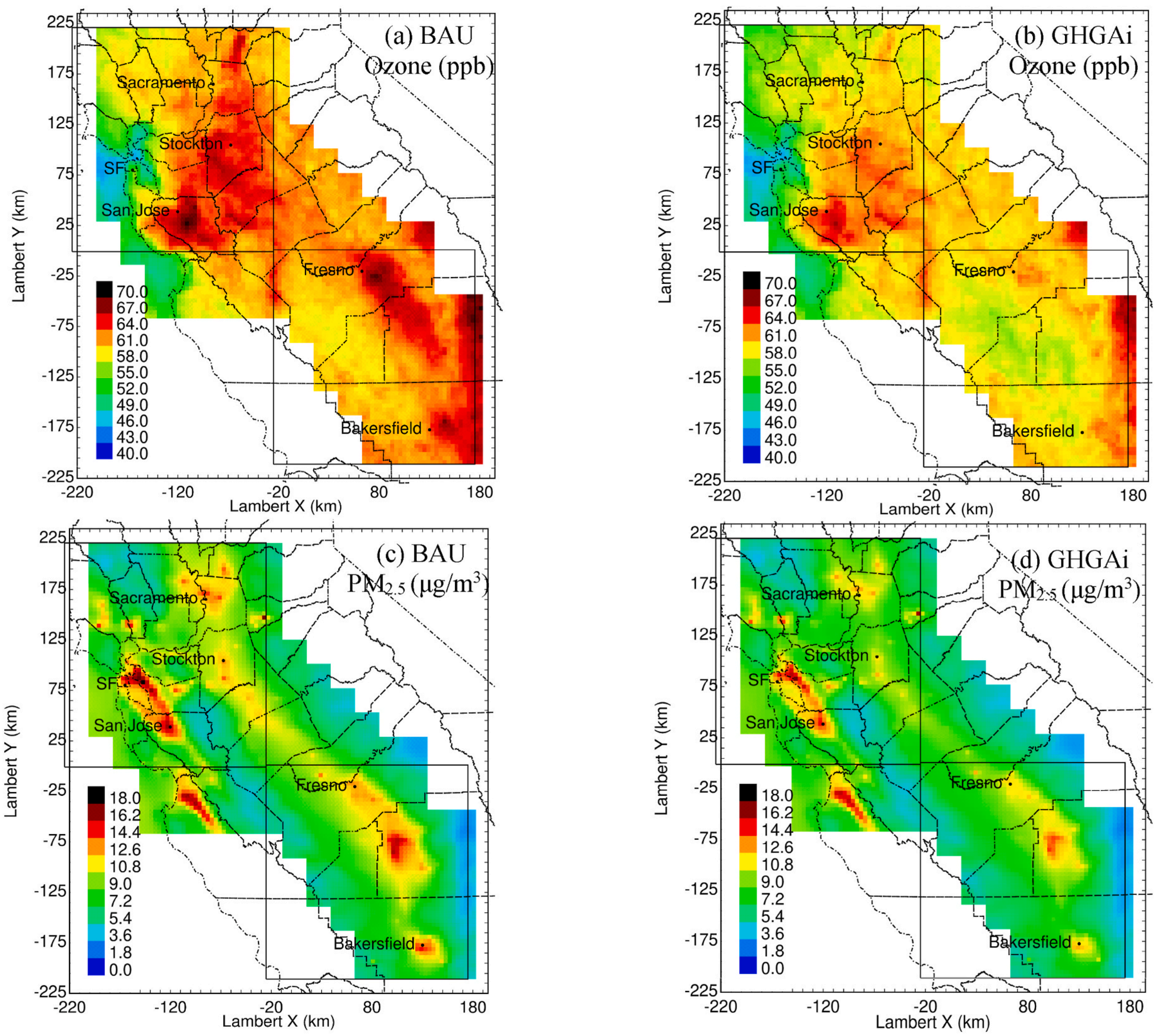

Fig. 1. Baseline concentrations among 32 weeks simulations of (a) 99th percentile MDA8 O_3 (ppb) under a BAU regional energy scenario, (b) 99th percentile MDA8 O_3 under a GHGAi regional energy scenario, (c) total average $PM_{2.5}$ (μg/m^3) under a BAU regional energy scenario, (d) total average $PM_{2.5}$ (μg/m^3) under a GHGAi regional energy scenario. Domains used for exposure analysis outlined in black lines.

(Fig. S6). The positive O_3 response to increased NOx emission in the GHGAi regional energy scenario (Fig. 2 (g,h)) reflects a change in the atmospheric chemical regime compared to the conditions in the BAU regional energy scenario (Fig. 2 (e,f)). This change in chemical regime is mainly associated with changes to emissions from non-dairy sources between the BAU and GHGAi regional energy scenario. The absolute magnitude of the change in O_3 concentrations is very small in both cases, leading to the conclusion that modern biogas engines emit sufficiently low quantities of NOx that they will have minor impacts on ambient O_3 concentrations in the SJV. Never-the-less, NOx emissions should be minimized where possible in any region out of compliance with National Ambient Air Quality Standards.

3.1.3. Particulate Matter response

Fig. 3 shows the difference in the long-term average $PM_{2.5}$ concentrations under various dairy scenarios relative to the baseline concentrations. Spatial patterns are illustrated for total $PM_{2.5}$ mass, $PM_{2.5}$ nitrate, and $PM_{2.5}$ OC. Patterns for other species are shown in SI.

Fig. 3 (a,b,c) shows the difference in the total average $PM_{2.5}$ concentrations due to adoption of the Perfect-Control scenario in the BAU regional energy scenario. Total $PM_{2.5}$ concentrations decrease by a maximum of 0.61 μg/m^3 when dairy waste emissions are eliminated, primarily due to the reduction in OC and other primary PM dominated by dust emissions. This indicates that over half of the emissions changes are associated with reductions in primary dust from animals walking in dairy freestall barns and adjacent drylot corrals. It is unlikely that Perfect-Control applied to dairy freestall barns and adjacent drylot corrals will reduce dust emissions by 100%, meaning that the $PM_{2.5}$ reductions illustrated in Fig. 3 will likely not be achievable in real-world applications.

It should be noted that NH_3 emissions were also eliminated from dairy waste emissions, but excess NH_3 from other agricultural sources in the SJV are sufficient to neutralize all available nitric acid. While there is a general decrease in nitrate concentrations, we observed a slight increase in $PM_{2.5}$ nitrate levels within the SJV, same as $PM_{2.5}$ ammonium concentrations. To understand the cause of this slight increase, a sensitivity analysis is performed where only VOC emissions were removed, keeping the NH_3 emissions consistent with the baseline scenario (Fig. S10). In this analysis, we also observe a slight rise in nitrate, ammonium and sulfate levels within the SJV, which suggests that the increase is primarily due to a shift in the atmospheric chemical regime in the region. A significant portion of the VOCs from dairy emissions are alkane species (Table 3: CH4, ALK1, ALK2, ALK3, ALK4), which react relatively slowly (and exclusively) with OH in the atmosphere. These species likely act as a sink for OH, and their elimination might potentially leading to an enhanced formation of secondary PM species.

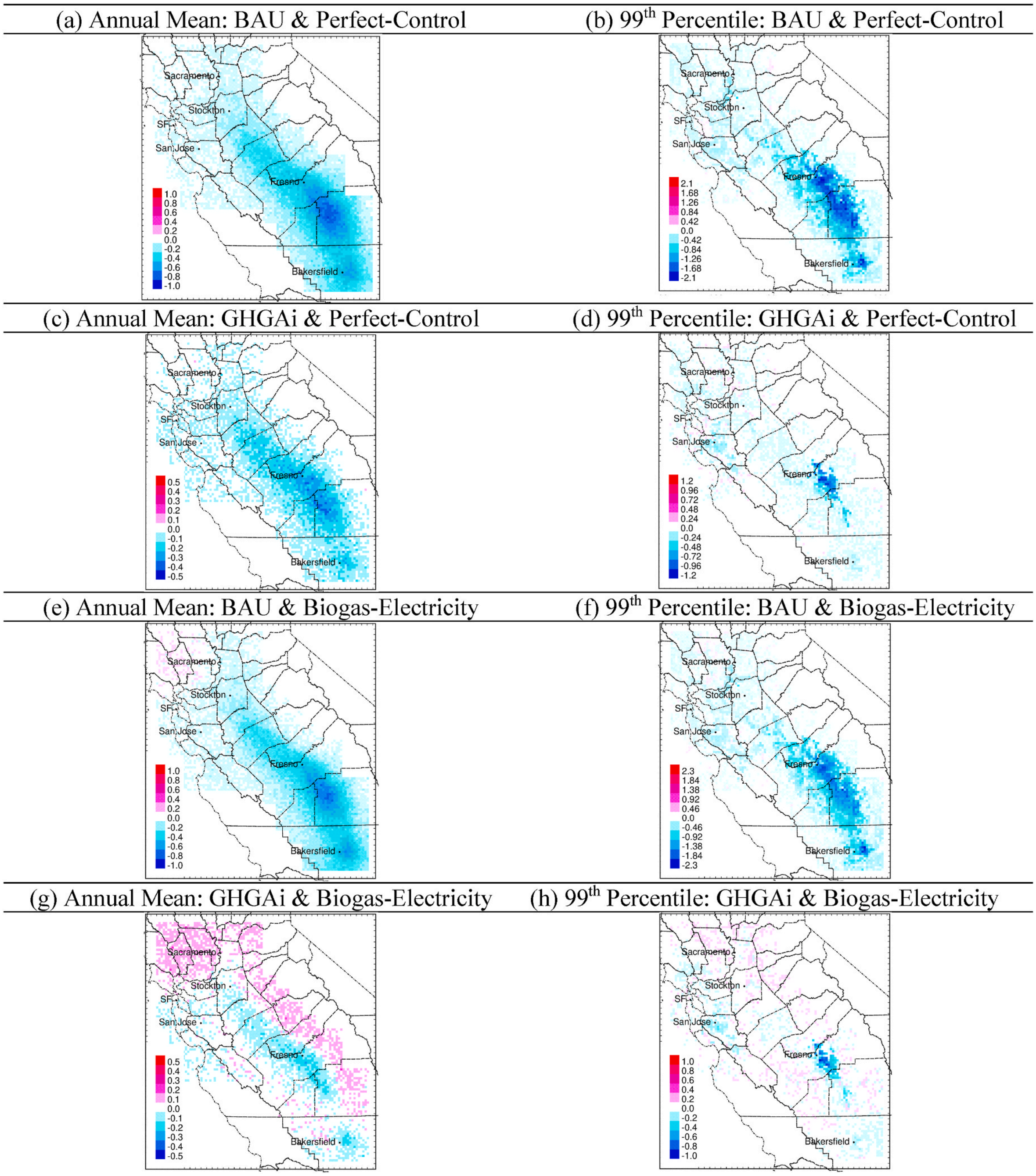

Fig. 2. Changes in MDA8 O_3 concentration (ppb) under various future scenarios. Negative values indicate reduced O_3 concentration under the scenario vs. the baseline case. Left column shows annual mean MDA8 O_3 concentration; Right column shows the 99th percentile MDA8 O_3 concentration.

Ultimately, the rise in secondary $PM_{2.5}$ species within the SJV is negligible, especially when contrasted with the reduction of primary $PM_{2.5}$ species, which results in a net decrease across the SJV and the entire mapped area.

Fig. 3 (d,e,f) show the changes in long-term average $PM_{2.5}$ concentrations predicted in response to the adoption of a Perfect-Control scenario in a GHGAi regional energy scenario. The spatial pattern and magnitude of the changes in $PM_{2.5}$ concentrations are almost identical in the GHGAi regional energy scenario (Fig. 3 (d,e,f)) and the BAU regional energy scenario (Fig. 3 (a,b,c)) because the atmospheric chemical regime has very little influence on the primary PM components that drive most of the changes.

Fig. 3 (g,h,i) illustrate predicted changes to long-term average $PM_{2.5}$ concentrations in response to the adoption of Biogas-Electricity in the SJV under a BAU regional energy scenario. Minor increases in $PM_{2.5}$ nitrate concentrations of 0.07 $\mu g/m^3$ are predicted in the SJV in response to increased NOx emissions from biogas combustion to produce electricity. The Biogas-Electricity scenario assumes that NH_3 and PM emissions from dairies are unchanged, and so the reductions in $PM_{2.5}$ OC in the SJV that are significant in the Perfect-Control scenario (Fig. 3c) are absent in the Biogas-Electricity scenario (Fig. 3i). It is evident that the utilization of biogas engines will result in a very minor increase in the overall $PM_{2.5}$ concentrations in the SJV (mostly $PM_{2.5}$ nitrate), accompanied by a similarly minor rise in the Sacramento region. The maximum increase in total $PM_{2.5}$ is 0.06 $\mu g/m^3$ relative to the baseline concentration field.

Holly et al. (2017) measured ammonia emissions from digested and separated dairy manure during storage and after land application. The

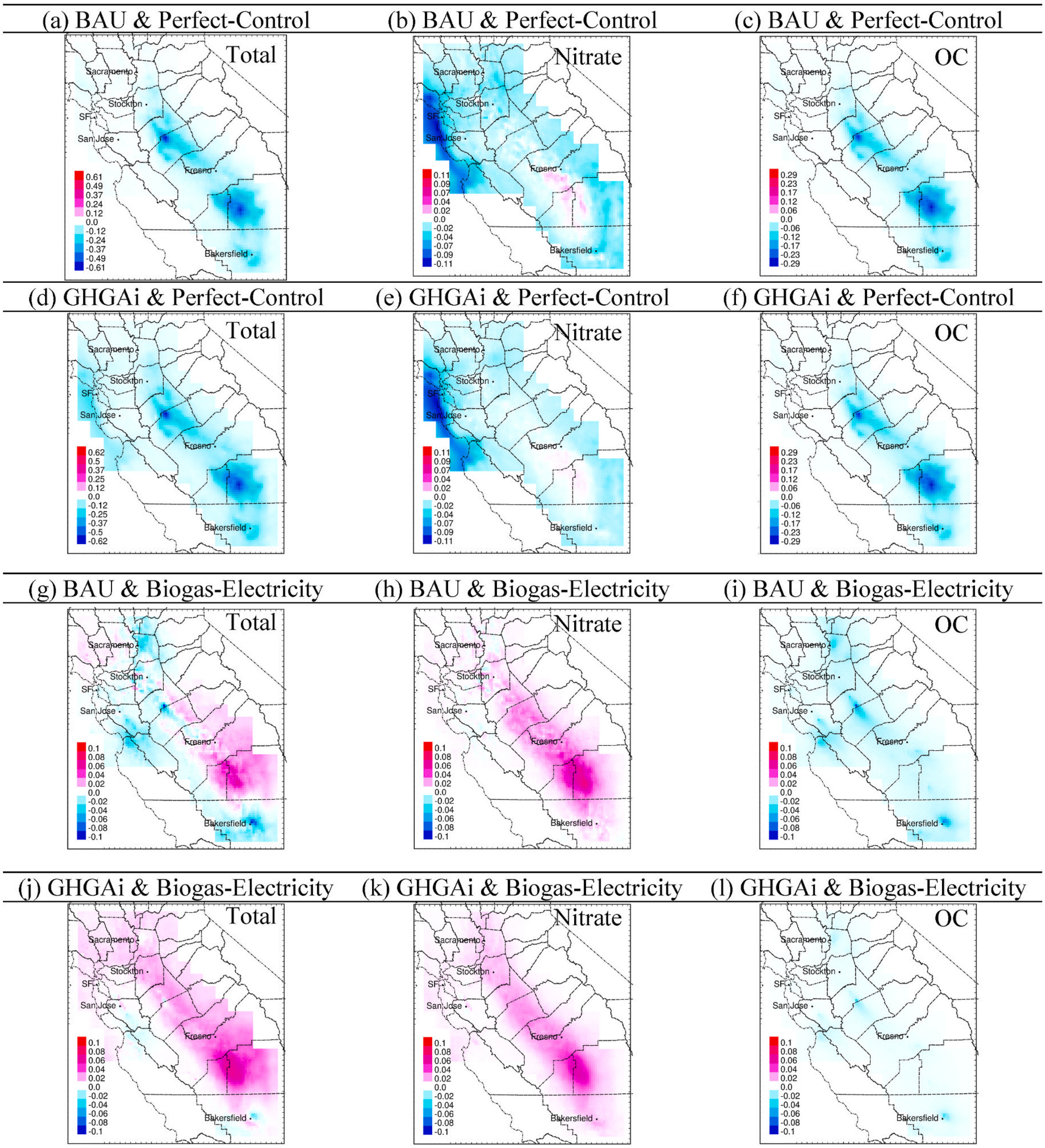

Fig. 3. Changes in annual average $PM_{2.5}$ concentrations (μg/m^3) under various scenarios. Negative values indicate reduced $PM_{2.5}$ concentration under the scenario vs. the baseline case, while positive values indicate increased $PM_{2.5}$ concentration. All results are averaged across the 32 weeks simulations.

authors concluded that anaerobic digestion significantly increased total ammonia emissions during storage in the absence of aggressive solid-liquid-separation measures and/or storage covers. Even if NH_3 emissions increase due to the widespread adoption of digesters, the impacts of potential increasing NH_3 emissions are modest in the SJV given the excess NH_3 that already exists in the atmosphere. One set of additional model simulations was conducted in the current study to consider the effects of a potential 40% increase in NH_3 emissions under the Biogas-Electricity scenario in a BAU regional energy scenario. Increasing NH_3 emission slightly increased predicted concentrations of average regional $PM_{2.5}$ by a maximum value of 0.03 μg/m^3 (Fig. S12). Increasing NH_3 emissions had no effect on predicted O_3 concentrations (Fig. S4). This sensitivity analysis suggests that the increases in NH_3 emissions due to the widespread adoption of anaerobic digesters will have minor impacts on air quality.

Fig. 3 (j,k,l) shows predicted changes in long-term average $PM_{2.5}$ concentrations in the Biogas-Electricity scenario under a GHGAi regional energy scenario. As expected, changes to primary $PM_{2.5}$ components are minimal due to the emissions of primary PM from biogas engines. The minor reduction in NOx emission from traditional natural gas sources compared to the BAU regional energy scenario further moderates the reduction in $PM_{2.5}$ OC. Certain areas that previously demonstrated slightly negative changes in the BAU regional energy & Biogas-Electricity scenario exhibit slightly positive changes in the GHGAi regional energy & Biogas-Electricity scenario, but all concentration changes are minor.

4. Public health impact

O_3 and $PM_{2.5}$ are significant air pollutants that have considerable impact on human health, primarily causing respiratory and cardiovascular issues. Exposure to O_3 is recognized to cause inflammation and irritation in the respiratory tract tissues, leading to symptoms such as coughing, chest tightness, and exacerbation of symptoms (Arjomandi et al., 2015; Golden et al., 1978; Zhang et al., 2019). Furthermore, long-term exposure to O_3 is linked to higher chances of cardiovascular and respiratory mortality (Jerrett et al., 2009; Nuvolone et al., 2018; Turner et al., 2016; Wang et al., 2020). Likewise, elevated levels of $PM_{2.5}$ are linked to premature death (Dominici et al., 2006; Laden et al., 2006; Pope III et al., 2002), increased cancer risk (Hamra et al., 2014) and impairment in the lung development in children (Gauderman et al., 2004). Exposure to $PM_{2.5}$ for an extended duration results in both immediate health problems and long-term consequences (Kelly and Fussell, 2015; Shi et al., 2016), contributing to reduced life expectancy and increased healthcare costs (Brook et al., 2010; Fann et al., 2018; Pope III et al., 2019).

4.1. Overall health co-benefits

The long-term O_3 and $PM_{2.5}$ health effects of the biogas electricity generation on mortality in the modeled region were evaluated using the BenMAP-Community Edition v1.5 model maintained by the US EPA (Sacks et al., 2018). Fig. 4 shows the changes of mortality associated with different treatments of dairy emissions per 100,000 population in BAU and GHGAi regional energy scenarios. The population data used in BenMAP is processed using PopGrid, an EPA-approved software program that generates population datasets at self-defined grids for BenMap analysis. Population is used as a spatial surrogate to describe where emissions occur within a larger geographic unit such as a county. It is important that the population fields used to describe emissions are identical to population used to calculate air pollution exposure to avoid any structural bias in the calculated health impacts. The CA-TIMES and CA-REMARQUE emissions inventories were constructed using 2010 population fields projected to 2050 using estimates from the California Department of Finance. BenMap calculations were performed with compatible 2010 census data (Sacks et al., 2018). Results are expressed as excess deaths per 100,000 residents to remove uncertainty about the total population rather than the spatial distribution of the population.

The O_3 health impact function is based on the study of Turner et al. (2016), and the O_3 indicator used for BenMAP analysis is the annual mean MDA8 O_3 (ppb). The $PM_{2.5}$ health impact function was taken to be an evenly weighted average of four independent epidemiological studies (Krewski et al., 2009; Laden et al., 2006; Lepeule et al., 2012; Pope III et al., 2002), and the annual mean $PM_{2.5}$ ($\mu g/m^3$) is used as indicator. Changes of mortality are translated to public health benefits using the standard value of a statistical life (VSL) recommended by US EPA, \$7.8M (2015\$).

In the case of O_3, all scenarios demonstrate mortality reductions. The Perfect-Control scenario has approximately 0.2 per 100,000 population in the BAU regional energy scenario, while the other biogas scenarios achieve slightly smaller reductions. Under the GHGAi regional energy scenario, the reduction is around 0.1 per 100,000 population for the Perfect-Control scenario and the reduction in the Biogas-Electricity scenario is minor. Regarding $PM_{2.5}$, the Perfect-Control scenario reduced mortality by approximately 0.5–0.6 per 100,000 population in both regional energy scenarios. The Biogas-Electricity and Biogas-Electricity-1.4NH3 with enhanced NH_3 production scenarios decrease mortality by a very small amount (less than 0.04 per 100,000 population) in the BAU regional energy scenario. Biogas electricity generation under the GHGAi regional energy scenario has a minor increase in mortality for $PM_{2.5}$ (less than 0.1 per 100,000 population).

In both the BAU and GHGAi regional energy scenarios, the Perfect-Control scenario defines the maximum hypothetical health benefit. It should be noted that the Perfect-Control scenario is unrealistic and is only provided to identify limiting conditions in the current study. Notably, even within this Perfect-Control scenario, the observed reduction in mortality remains almost negligibly small, not exceeding 1 per 100,000 population. Likewise, the monetary value of the maximum health co-benefits are limited, amounting to less than 7 million per 100,000 population. This suggests that while the adoption of biogas electricity presents certain trade-offs, the overall impact on mortality rates per 100,000 individuals, particularly concerning O_3 and $PM_{2.5}$ exposure, is small. The lack of significant variance across different dairy scenarios suggests that biogas electricity generation has a negligible impact on O_3 and $PM_{2.5}$ mortality changes within the studied regions.

4.2. Race/ethnicity disparities

California is at the forefront of the national environmental justice (EJ) movement (Anderson et al., 2018; Morello-Frosch et al., 2002; Pastor et al., 2005). Extensive EJ research indicates that socio-economically disadvantaged groups in the U.S. are exposed to higher levels of air pollution, a disparity arising from numerous historical policies (Miranda et al., 2011; Schlosberg, 2004). In this setting, it is imperative to consider the potential EJ impacts of any changes that may alter air pollution patterns in California.

Air pollution exposure is calculated and EJ is analyzed for different race/ethnicity groups using the socio-economic data from the American Community Survey (ACS) 2012–2016 (United State Census Bureau, 2020). In this study, two regions that cover population centers were selected: the SJV and the combined Bay Area & Sacramento (Bay & Sac), as defined in Fig. 1. Table 4 shows the ethnicity distribution in the SJV

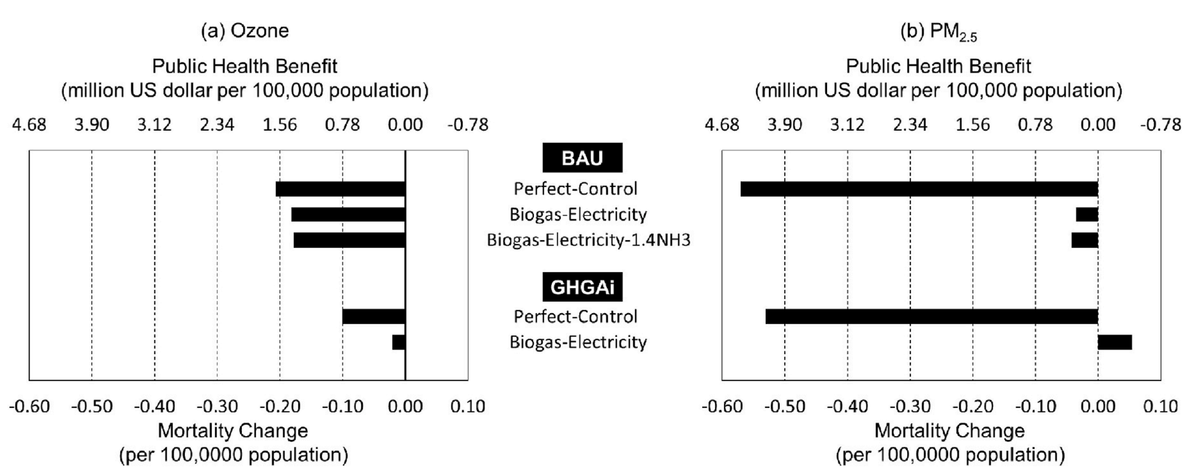

Fig. 4. The change of mortality and public health benefit per 100,000 population associated with dairy scenarios (relative to the baseline scenario) in Central (SJV) and Northern (Bay & Sac) California, (a) O_3 (annual mean MDA8 O_3), (b) $PM_{2.5}$.

Table 4
Scenarios Socio-economic data from American Community Survey (ACS) 2012–2016.

Race/Ethnicity[a]	Population		Percentage	
	SJV	Bay & Sac	SJV	Bay & Sac
All	2191214	10484207		
Black	91525	619651	4.18%	5.91%
Hispanic	1252397	2725409	57.16%	26.00%
Asian	143476	2124764	6.55%	20.27%
White	661816	4541562	30.20%	43.32%

[a] Black: Black and African American; Hispanic: Hispanic or Latino, regardless of races; Asian: Asian Alone; White: Non-Hispanic White.

and the Bay & Sac areas. Hispanic residents account for 57.16% of the total population in the SJV. White residents account for 43.32% of the population in the Bay & Sac region. The Asian population is 20.27% of the total in the Bay & Sac, and 6.55% in the SJV. The Black and African American population is 5.91% in the Bay & Sac region and 4.18% in the SJV.

Figs. 5 and 6 illustrate the future year 2050 population weighted concentrations (PWC) of O_3 (ppb) and $PM_{2.5}$ ($\mu g/m^3$) as well as the exposure disparity for race/ethnicity groups in the SJV and Bay & Sac areas. As suggested by EPA (EPA, 2019), the O_3 indicator used for the EJ analysis is the average of the top ten MDA8 O_3 concentrations (above 96th percentile), while the $PM_{2.5}$ indicator is the annual average. The regulatory O_3 exposure metric based on the 99th percentile concentration averaged over three years follows the same trends as the 96th percentile O_3 concentration. Relative exposure disparity greater than zero indicates greater-than-average exposure, while exposure disparity less than zero indicates less-than-average exposure.

While there is a consistently elevated level of O_3 in the SJV compared to the Bay & Sac region especially in the BAU regional energy scenario, the racial/ethnic disparity in O_3 (Fig. 5) exposure varies largely between the two regions under investigation. Within the SJV, Asian residents consistently have above-average O_3 exposure across all emission and dairy scenarios. Conversely, all other race/ethnicity groups experience O_3 exposure levels that are near the average: White residents face slightly worse than average levels, while Black and non-white Hispanic residents experience somewhat lower levels of O_3 exposure. In the Bay & Sac region, there is a smaller race/ethnicity discrepancy. Non-white Hispanic residents have the highest exposure to O_3, while Black and African residents have the lowest exposure to O_3.

In the case of $PM_{2.5}$ (Fig. 6), the levels of $PM_{2.5}$ exposure disparities in the Bay & Sac region are generally higher than those in the SJV, and the racial/ethnic disparity appears to be more similar compared to that observed for O_3. White residents consistently experience lower-than-average exposure levels in both locations across all emission scenarios considered in the current study. Conversely, Black &African American residents along with Asian residents, experience the highest $PM_{2.5}$ concentrations. Non-white Hispanic individuals experience slightly lower-than-average $PM_{2.5}$ exposure in the SJV and slightly higher-than-average exposure in the Bay & Sac region.

The variation in exposure disparities to ozone O_3 and $PM_{2.5}$ across different racial groups has been reported by other studies (Collins et al., 2022). These patterns largely reflect the proximity of each

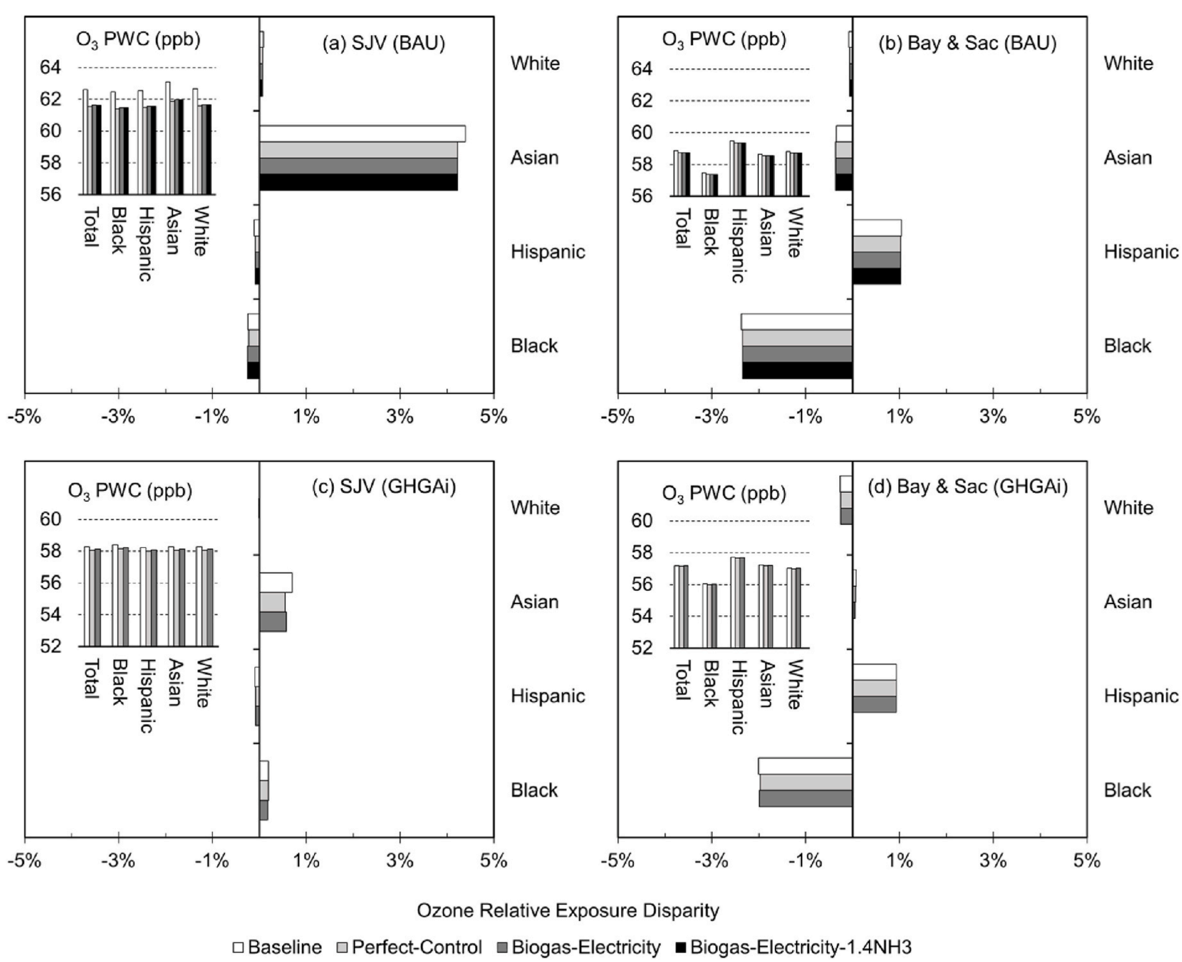

Fig. 5. Future year (2050) O_3 PWC (ppb) and exposure disparity by scenarios and race/ethnicity: (a) SJV in a BAU regional energy scenario, (b) SJV in a GHGAi regional energy scenario, (c) Bay & Sac in a BAU regional energy scenario (d) Bay & Sac in a GHGAi regional energy scenario.

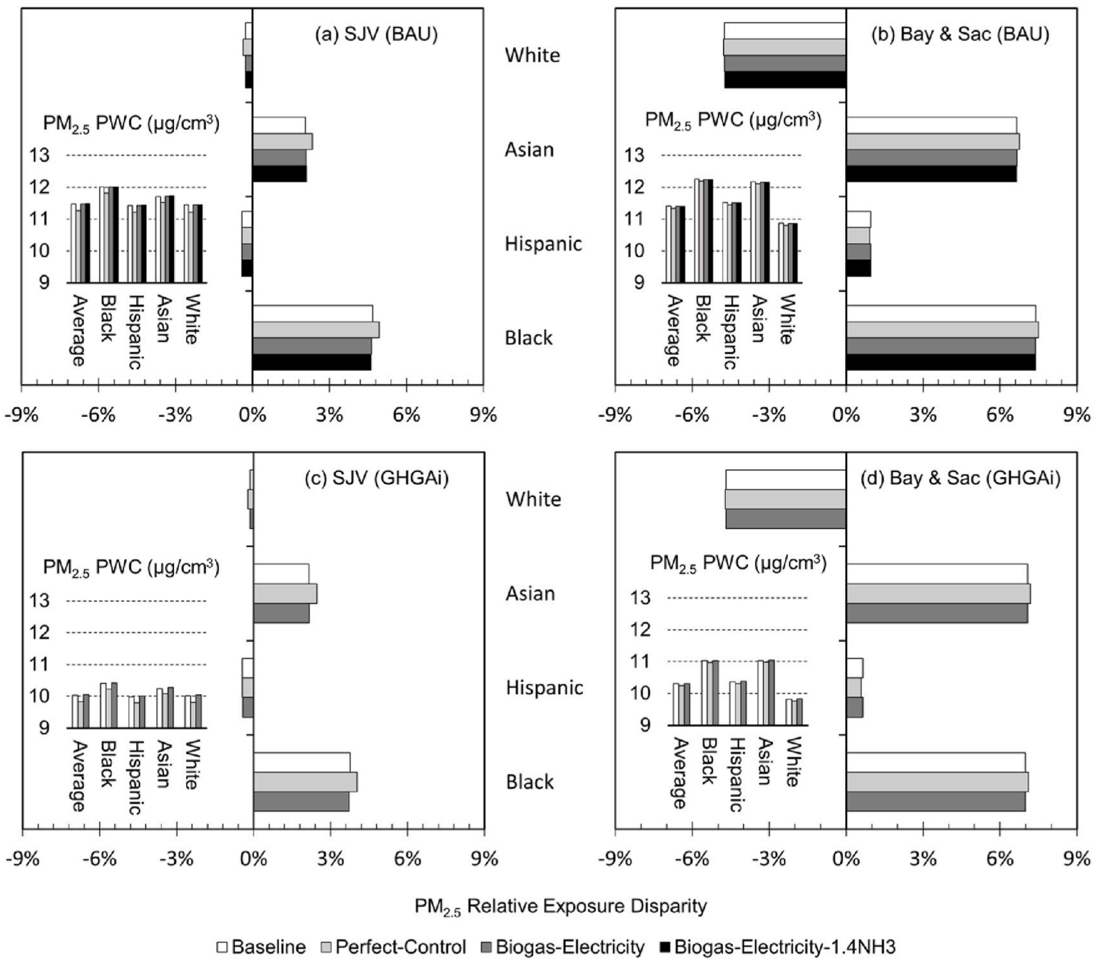

Fig. 6. Future year (2050) $PM_{2.5}$ PWC (μg/cm^3) and exposure disparity by scenarios and race/ethnicity: (a) SJV in a BAU regional energy scenario, (b) SJV in a GHGAi regional energy scenario, (c) Bay & Sac in a BAU regional energy scenario (d) Bay & Sac in a GHGAi regional energy scenario.

race/ethnicity group to the urban core of the major cities in each region (Li et al., 2022a). White residents are more dispersed in suburban neighborhoods that are further away from urban cores that have lower-than-average primary air pollution exposures. Black &African American residents in California are clustered into neighborhoods near the center of urban cores or near major transportation corridors, where there is a larger concentration of primary air pollution emissions (Fig. S7 & Fig. S8). In the Bay & Sac region, those urban cores are under NOx-rich chemical conditions (Fig. S15), resulting in relatively low level of O_3 for the Black and African American residents. The Bay & Sac areas also have a much larger Asian population compared to the SJV. This disparity may be attributed to the concentration of Asian residents in urban cores, particularly within major cities such as downtown San Francisco and San Jose.

Regardless of the regional energy scenarios (BAU or GHGAi), the adoption of biogas electricity production has minimal impact on exposure disparities in either the SJV or the Bay & Sac regions, from both O_3 and $PM_{2.5}$ EJ analysis. Exposure disparity changes are negligible when comparing the Biogas-Electricity scenario to the baseline scenario. Even the Perfect-Control scenario has little impact on exposure disparities in the study region because the rural dairy farms are generally located far from the population centers. It should be noted that other forms of biogas adoption (transportation fuel or pipeline injection) will have even less environmental impact than the bounding scenarios analyzed in the current study. These results indicate that EJ concerns are not a dominant factor when deciding whether to adopt biogas electricity production in central California.

5. Conclusion

Dairy waste emissions in the SJV make minor contributions to regional O_3 and $PM_{2.5}$ concentrations. A hypothetical Perfect-Control scenario involving complete elimination of all emissions from dairy waste would only reduce annual average MDA8 O_3 concentrations in the SJV by about 1~2 ppb and total $PM_{2.5}$ concentrations by ~0.6 μg/m^3 compared to baseline conditions in the year 2050.

Widespread adoption of biogas production from dairy waste and combustion to replace 80 MW of fossil natural gas electricity generation with biogas electricity generation reduces GHG emissions from the agricultural sector with minimal impact on air pollution. Even in the most extreme scenario involving 100% local electricity production in the SJV, biogas adoption results in only minor increases in population-weighted O_3 and $PM_{2.5}$ levels across the region. Notably, the NOx emissions from biogas combustion marginally increase secondary $PM_{2.5}$ nitrate concentrations by less than 0.1 μg/m^3 and have a mixed effect on MDA8 O_3 concentrations depending on the VOC- or NOx-limited nature of the atmosphere. The primary PM emissions from biogas production facilities are negligible in their impact on regional $PM_{2.5}$ concentrations. Other forms of biogas adoption involving upgrading gas for use as a transportation fuel or for pipeline injection would have even less impact on regional air quality.

Dairy digesters are unlikely to significantly influence future compliance with National Ambient Air Quality Standards for O_3 and $PM_{2.5}$ in the SJV or the Bay & Sac regions. Widespread biogas electricity production would change air pollution mortality by less than 0.1 excess death per 100,000 population. If future regional conditions are NOx-rich, biogas electricity production slightly reduces $PM_{2.5}$ and O_3 concentrations. If future regional conditions are NOx-limited, then biogas electricity production slightly increases $PM_{2.5}$ and slightly reduces O_3 concentrations. The magnitude of the change in public health risk is minor in either case. For comparison, the public health risk for seasonal flu/pneumonia in California is approximately 10.5 excess deaths per 100,000 population (CDC, 2021), which is more than 100 times larger than any positive or negative change induced by biogas electricity production. EJ analysis reveals that the adoption of digesters also does not affect exposure disparities among different racial groups in both the SJV and the Bay & Sac area.

The science-based strategies to address air pollution and climate change that are developed in California are often adopted in neighboring states and countries. California's commitment to a weight-of-evidence approach has yielded successful strategies that have improved air quality and reduced GHG emissions across the state and the world for the past five decades. Looking forward, adoption of dairy digesters to control methane emissions from agricultural sources appears to be an effective method to reduce GHG emissions with minimal impact on surrounding air quality.

CRediT authorship contribution statement

Jia Jiang: Writing – original draft, Formal analysis. **Yiting Li:** Methodology, Investigation. **Michael Kleeman:** Writing – review & editing, Supervision, Software, Project administration, Funding acquisition, Formal analysis, Conceptualization.

Declaration of competing interest

The authors declare that they have no known competing financial interests or personal relationships that could have appeared to influence the work reported in this paper.

Data availability

Data will be made available on request.

Acknowledgement

This research was funded by CARB under Project 17RD017. The statements and conclusions in this work are those of the authors and not necessarily those of CARB.

Appendix A. Supplementary data

Supplementary data to this article can be found online at https://doi.org/10.1016/j.atmosenv.2024.120588.

References

Akherati, A., Cappa, C.D., Kleeman, M.J., Docherty, K.S., Jimenez, J.L., Griffith, S.M., Dusanter, S., Stevens, P.S., Jathar, S.H., 2019. Simulating secondary organic aerosol in a regional air quality model using the statistical oxidation model – Part 3: Assessing the influence of semi-volatile and intermediate volatility organic compounds and NOX. Atmos. Chem. Phys. 19, 4561–4594.

Anderson, C.M., Kissel, K.A., Field, C.B., Mach, K.J., 2018. Climate change mitigation, air pollution, and environmental justice in California. Environ. Sci. Technol. 52, 10829–10838. https://doi.org/10.1021/acs.est.8b00908.

Anenberg, S.C., Schwartz, J., Shindell, D., Amann, M., Faluvegi, G., Klimont, Z., Janssens-Maenhout, G., Pozzoli, L., Van Dingenen, R., Vignati, E., Emberson, L., 2012. Global air quality and health co-benefits of mitigating near-term climate change through methane and black carbon emission controls. Environ. Health Perspect. 120 (6), 831–839. https://doi.org/10.1289/ehp.1104301.

Arjomandi, M., Wong, H., Donde, A., Frelinger, J., Dalton, S., Ching, W., Power, K., Balmes, J.R., 2015. Exposure to medium and high ambient levels of ozone causes adverse systemic inflammatory and cardiac autonomic effects. Am. J. Physiol. Heart Circ. Physiol. 308, H1499–H1509. https://doi.org/10.1152/ajpheart.00849.2014.

Brook, R.D., Rajagopalan, S., Pope 3rd, C.A., Brook, J.R., Bhatnagar, A., Diez-Roux, A.V., Holguin, F., Hong, Y., Luepker, R.V., Mittleman, M.A., Peters, A., Siscovick, D., Smith Jr., S.C., Whitsel, L., Kaufman, J.D., American Heart Association Council on, E., Prevention, C.o.t.K.i.C.D., Council on Nutrition, P.A., Metabolism, 2010. Particulate matter air pollution and cardiovascular disease: an update to the scientific statement from the American Heart Association. Circulation 121, 2331–2378. https://doi.org/10.1161/CIR.0b013e3181dbece1.

CARB, 2015. California's methane inventory based on the 2015 edition the CARB greenhouse gas inventory. Retrieved from. https://ww2.arb.ca.gov/ghg-slcp-inventory.

Carter, W.P.L., Heo, G., 2013. Development of revised SAPRC aromatics mechanisms. Atmos. Environ. 77, 404–414. https://doi.org/10.1016/j.atmosenv.2013.05.021.

CDC, 2021. Influenza and pneumonia deaths. https://www.cdc.gov/nchs/pressroom/sosmap/flu_pneumonia_mortality/flu_pneumonia.htm.

CDFA, 2018. California dairy statistics annual 2017 Data. https://www.cdfa.ca.gov/dairy/pdf/Annual/2017/2017_Statistics.Annual.pdf.

CDFA, 2019. California agricultural statistics review. https://www.cdfa.ca.gov/statistics/PDFs/2018-2019AgReportnass.pdf.CDFA.

Collins, T.W., Grineski, S.E., Nadybal, S.M., 2022. A comparative approach for environmental justice analysis: Explaining divergent societal distributions of particulate matter and ozone pollution across US neighborhoods. Ann. Assoc. Am. Geogr. 112 (2), 522–541. https://doi.org/10.1080/24694452.2021.1935690.

Dominici, F., Peng, R.D., Bell, M.L., Pham, L., McDermott, A., Zeger, S.L., Samet, J.M., 2006. Fine particulate air pollution and hospital admission for cardiovascular and respiratory diseases. JAMA 295, 1127–1134. https://doi.org/10.1001/jama.295.10.1127.

El Mashad, H.M., Barzee, T.J., Franco, R.B., Zhang, R., Kaffka, S., Mitloehner, F., 2023. Anaerobic digestion and Alternative manure Management technologies for methane emissions mitigation on Californian dairies. Atmosphere 14, 120.

Emery, C., Liu, Z., Russell, A.G., Odman, M.T., Yarwood, G., Kumar, N., 2017. Recommendations on statistics and benchmarks to assess photochemical model performance. J. Air Waste Manag. Assoc. 67 (5), 582–598. https://doi.org/10.1080/10962247.2016.1265027.

EPA, U.S, 2016. Nonroad Compression-Ignition Engines: Exhaust Emission Standards. https://nepis.epa.gov/Exe/ZyPDF.cgi?Dockey=P100OA05.pdf.

Epa, U.S., 2019. Overview of environmental indicators in EJScreen. https://www.epa.gov/ejscreen/overview-environmental-indicators-ejscreen.

Fann, N., Coffman, E., Timin, B., Kelly, J.T., 2018. The estimated change in the level and distribution of PM(2.5)-attributable health impacts in the United States: 2005-2014. Environ. Res. 167, 506–514. https://doi.org/10.1016/j.envres.2018.08.018.

Fiore, A.M., Jacob, D.J., Field, B.D., Streets, D.G., Fernandes, S.D., Jang, C., 2002. Linking ozone pollution and climate change: the case for controlling methane. Geophys. Res. Lett. 29 (19) https://doi.org/10.1029/2002GL015601, 25-1.

Gauderman, W.J., Avol, E., Gilliland, F., Vora, H., Thomas, D., Berhane, K., McConnell, R., Kuenzli, N., Lurmann, F., Rappaport, E., Margolis, H., Bates, D., Peters, J., 2004. The effect of air pollution on lung development from 10 to 18 years of age. N. Engl. J. Med. 351, 1057–1067. https://doi.org/10.1056/NEJMoa040610.

Giorgi, F., Meleux, F., 2007. Modelling the regional effects of climate change on air quality. Compt. Rendus Geosci. 339 (11–12), 721–733. https://doi.org/10.1016/j.crte.2007.08.006.

Golden, J.A., Nadel, J.A., Boushey, H.A., 1978. Bronchial hyperirritability in healthy subjects after exposure to ozone. Am. Rev. Respir. Dis. 118, 287–294. https://doi.org/10.1164/arrd.1978.118.2.287.

Hamra, G.B., Guha, N., Cohen, A., Laden, F., Raaschou-Nielsen, O., Samet, J.M., Vineis, P., Forastiere, F., Saldiva, P., Yorifuji, T., Loomis, D., 2014. Outdoor particulate matter exposure and lung cancer: a systematic review and meta-analysis. Environ. Health Perspect. 122, 906–911. https://doi.org/10.1289/ehp/1408092.

Holly, M.A., Larson, R.A., Powell, J.M., Ruark, M.D., Aguirre-Villegas, H., 2017. Greenhouse gas and ammonia emissions from digested and separated dairy manure during storage and after land application. Agric. Ecosyst. Environ. 239, 410–419. https://doi.org/10.1016/j.agee.2017.02.007.

Hu, J., Zhang, H., Ying, Q., Chen, S., Vandenberghe, F., Kleeman, M.J., 2015. Long-term particulate matter modeling for health effects studies in California – Part I: model performance on Temporal and spatial variations. Atmos. Chem. Phys. 15 (6), pp3445–3461.

Hu, J., Jathar, S., Zhang, H., Ying, Q., Chen, S., Cappa, C.D., Kleeman, M.J., 2017. Long-term particulate matter modeling for health effect studies in California – Part 2: concentrations and sources of ultrafine organic aerosols. Atmos. Chem. Phys. 17, 5379–5391. https://doi.org/10.5194/acp-17-5379-2017.

Hu, J., Ostro, B., Zhang, H., Ying, Q., Kleeman, M.J., 2019. Using chemical transport model Predictions to Improve exposure Assessment of PM2.5 Constituents. Environ. Sci. Technol. Lett. 6, 456–461.

IEA, 2021. Methane Tracker 2021. IEA, Paris.

Jerrett, M., Burnett, R.T., Pope 3rd, C.A., Ito, K., Thurston, G., Krewski, D., Shi, Y., Calle, E., Thun, M., 2009. Long-term ozone exposure and mortality. N. Engl. J. Med. 360, 1085–1095. https://doi.org/10.1056/NEJMoa0803894.

Jerrett, M.J., Nau, C.L., Young, D.R., Butler, R.K., Batteate, C.M., Padilla, A., Tartof, S.Y., Su, J., Burnett, R.T., Kleeman, M.J., 2023. Air pollution and the Sequelae of COVID-19 Patients: a Multistate analysis. Environ. Res. 236 (Pt 2), 116814 https://doi.org/10.1016/j.envres.2023.116814.

Kelly, F.J., Fussell, J.C., 2015. Air pollution and public health: emerging hazards and improved understanding of risk. Environ. Geochem. Health 37, 631–649. https://doi.org/10.1007/s10653-015-9720-1.

Krewski, D., Jerrett, M., Burnett, R.T., Ma, R., Hughes, E., Shi, Y., Turner, M.C., Pope III, C.A., Thurston, G., Calle, E.E., 2009. Extended Follow-Up and Spatial Analysis of the American Cancer Society Study Linking Particulate Air Pollution and Mortality.

Laden, F., Schwartz, J., Speizer, F.E., Dockery, D.W., 2006. Reduction in fine particulate air pollution and mortality: extended follow-up of the Harvard Six Cities study. Am. J. Respir. Crit. Care Med. 173, 667–672. https://doi.org/10.1164/rccm.200503-443OC.

Lepeule, J., Laden, F., Dockery, D., Schwartz, J., 2012. Chronic exposure to fine particles and mortality: an extended follow-up of the Harvard Six Cities study from 1974 to 2009. Environ. Health Perspect. 120, 965–970. https://doi.org/10.1289/ehp.1104660.

Li, Y., Kumar, A., Li, Y., Kleeman, M.J., 2022a. Adoption of low-carbon fuels reduces race/ethnicity disparities in air pollution exposure in California. Sci. Total Environ. 834, 155230 https://doi.org/10.1016/j.scitotenv.2022.155230.

Li, Y., Yang, C., Li, Y., Kumar, A., Kleeman, M.J., 2022b. Future emissions of particles and gases that cause regional air pollution in California under different greenhouse gas mitigation strategies. Atmos. Environ. 273, 118960 https://doi.org/10.1016/j.atmosenv.2022.118960.

Li, Y., Wang, G., Murphy, C., Kleeman, M.J., 2023. Modeling expected air quality impacts of Oregon's Proposed Expanded clean fuels program. Atmos. Environ. 296. ISSN 1352-2310.

Li, Y., Zhao, Kleeman, M.J., 2024. Formaldehyde exposure racial disparities in southeast Texas. Environ. Sci. Technol. 58 (10), pp4680–4690.

Miranda, M.L., Edwards, S.E., Keating, M.H., Paul, C.J., 2011. Making the environmental justice grade: the relative burden of air pollution exposure in the United States. Int. J. Environ. Res. Publ. Health 8, 1755–1771. https://doi.org/10.3390/ijerph8061755.

Mosavi, P., 2023. Manure, methane, and Money: the anaerobic digester Disaster in California. Anim. Law 29, 41.

Morello-Frosch, R., Pastor Jr., M., Porras, C., Sadd, J., 2002. Environmental justice and regional inequality in southern California: implications for future research. Environ. Health Perspect. 110 (Suppl. 2), 149–154. https://doi.org/10.1289/ehp.02110s2149.

Nuvolone, D., Petri, D., Voller, F., 2018. The effects of ozone on human health. Environ. Sci. Pollut. Res. Int. 25, 8074–8088. https://doi.org/10.1007/s11356-017-9239-3.

Pastor Jr., M., Morello-Frosch, R., Sadd, J.L., 2005. The air is always cleaner on the other side: race, space, and ambient air toxics exposures in California. J. Urban Aff. 27, 127–148. https://doi.org/10.1111/j.0735-2166.2005.00228.x.

Pope III, C.A., Burnett, R.T., Thun, M.J., Calle, E.E., Krewski, D., Ito, K., Thurston, G.D., 2002. Lung cancer, cardiopulmonary mortality, and long-term exposure to fine particulate air pollution. JAMA 287, 1132–1141. https://doi.org/10.1001/jama.287.9.1132.

Pope III, C.A., Lefler, J.S., Ezzati, M., Higbee, J.D., Marshall, J.D., Kim, S.-Y., Bechle, M., Gilliat, K.S., Vernon, S.E., Robinson, A.L., 2019. Mortality risk and fine particulate air pollution in a large, representative cohort of US adults. Environ. Health Perspect. 127, 077007 https://doi.org/10.1289/EHP4438.

Sacks, J.D., Lloyd, J.M., Zhu, Y., Anderton, J., Jang, C.J., Hubbell, B., Fann, N., 2018. The Environmental Benefits Mapping and Analysis Program - Community Edition (BenMAP-CE): a tool to estimate the health and economic benefits of reducing air pollution. Environ. Model. Software 104, 118–129. https://doi.org/10.1016/j.envsoft.2018.02.009.

Schlosberg, D., 2004. Reconceiving environmental justice: global movements and political theories. Environ. Polit. 13, 517–540. https://doi.org/10.1080/0964401042000229025.

Shi, L., Zanobetti, A., Kloog, I., Coull, B.A., Koutrakis, P., Melly, S.J., Schwartz, J.D., 2016. Low-concentration PM2.5 and mortality: Estimating Acute and Chronic effects in a population-based study. Environ. Health Perspect. 124, 46–52. https://doi.org/10.1289/ehp.1409111.

Staniaszek, Z., Griffiths, P.T., Folberth, G.A., O'Connor, F.M., Abraham, N.L., Archibald, A.T., 2022. The role of future anthropogenic methane emissions in air quality and climate. Npj Clim. Atmospheric Sci. 5 (1), 21. https://doi.org/10.1038/s41612-022-00247-5.

Turner, M.C., Jerrett, M., Pope 3rd, C.A., Krewski, D., Gapstur, S.M., Diver, W.R., Beckerman, B.S., Marshall, J.D., Su, J., Crouse, D.L., Burnett, R.T., 2016. Long-term ozone exposure and mortality in a large Prospective study. Am. J. Respir. Crit. Care Med. 193, 1134–1142. https://doi.org/10.1164/rccm.201508-1633OC.

Venecek, M.A., Cai, C., Kaduwela, A., Avise, J., Carter, W.P.L., Kleeman, M.J., 2018. Analysis of SAPRC16 chemical mechanism for ambient simulations. Atmos. Environ. 192, 136–150.

Venecek, M.A., Yu, X., Kleeman, M.J., 2019. Predicted ultrafine particulate matter source contributions across the continental United States during summer time air pollution events. Atmos. Chem. Phys. 19, 9399–9412.

Wang, Y., Wild, O., Chen, X., Wu, Q., Gao, M., Chen, H., Qi, Y., Wang, Z., 2020. Health impacts of long-term ozone exposure in China over 2013-2017. Environ. Int. 144, 106030 https://doi.org/10.1016/j.envint.2020.106030.

Yu, X., Venecek, M., Kumar, A., Hu, J., Tanrikulu, S., Soon, S., Tran, C., Fairley, D., Kleeman, M.J., 2019. Regional sources of airborne ultrafine particle number and mass concentrations in California. Atmos. Chem. Phys. 19, 14677–14702.

Zapata, C.B., Yang, C., Yeh, S., Ogden, J., Kleeman, M.J., 2018a. Estimating criteria pollutant emissions using the California regional multisector air quality emissions (CA-REMARQUE) model v1. 0. Geosci. Model Dev. (GMD) 11, 1293–1320.

Zapata, C.B., Yang, C., Yeh, S., Ogden, J., Kleeman, M.J., 2018b. Low-carbon energy generates public health savings in California. Atmos. Chem. Phys. 18, 4817–4830. https://doi.org/10.5194/acp-18-4817-2018.

Zhang, J.J., Wei, Y., Fang, Z., 2019. Ozone pollution: a major health Hazard Worldwide. Front. Immunol. 10, 2518. https://doi.org/10.3389/fimmu.2019.02518.

Zhao, Y., Li, Y., Kumar, A., Ying, Q., Vandenberghe, F., Kleeman, M.J., 2022. Separately resolving NOx and VOC contributions to ozone formation. Atmos. Environ. 285, 119224 https://doi.org/10.1016/j.atmosenv.2022.119224. ISSN 1352-2310.

Zhao, Y., Li, Y., Li, Y., Kumar, A., Ying, Q., Kleeman, M.J., 2023. Reducing southern California ozone concentrations in the Year 2050 under a low carbon energy scenario. Atmos. Environ. 320, 120315. ISSN 1352-2310.